Original Paper

phys. stat. sol. (a) **204** No. 8, 2555–2560 (2007) / **DOI** 10.1002/pssa.200675655

High-temperature induced nano-crystal formation in ion beam-induced amorphous silicon ripples

J. Grenzer [*, 1], **A. Mücklich**[1], **S. Grigorian** [2], **U. Pietsch**[2], **D. P. Datta**[3], **T. K. Chini**[3], **S. Hazra**[3], and **M. K. Sanyal**[3]

[1] Forschungszentrum Rossendorf, Institut für Ionenstrahlphysik und Materialforschung, P.O. Box 510119, 01314 Dresden, Germany
[2] University of Siegen, Institute of Physics, 57072 Siegen, Germany
[3] Surface Physics Division, Saha Institute of Nuclear Physics, 1/AF Bidhannagar, Kolkata 700 064, India

Received 8 October 2006, revised 12 January 2007, accepted 20 February 2007
Published online 1 August 2007

PACS 61.10.Nz, 61.82.Fk, 68.35.Fx, 68.37.Ps, 81.16.Rf

We report on in-situ investigations of a recrystallization process of amorphous and damaged crystalline parts generated during ion-beam induced rippling on a Si(100) surface. The ripple structure was created by 60 keV $^{40}Ar^{+}$ irradiation with a dose of $\sim 5 \times 10^{17}$ ions/cm^2 at ion incident angle of 60° with respect to the surface normal. At this dose the ripples have an average spatial periodicity of about 715 nm and surface undulations with an amplitude of about 40 nm. Structure and morphology of ripples were studied by two types of X-ray scattering (grazing incidence diffraction and amorphous scattering) methods, transmission electron microscopy and atomic force microscopy. X-ray grazing-incidence amorphous scattering pattern were recorded in-situ for a temperature range from 250 to 750 °C. Up to about 500 °C mainly we found a single broad scattering maximum corresponding to the Si(111) inter-planar distances. At higher temperature these peaks become sharp and intense indicating the onset of a re-crystallization process in the amorphous top layer.
Two processes were found, a formation of crystalline islands on top of the former amorphous surface ripples and a growth of polycrystalline twins close to the former amorphous-crystalline interface.

1 Introduction

The formation of periodic surface structures varying from several nm to a few μm caused by ion-beam sputter erosion processes on semiconductor surfaces has attracted significant interest for the fabrication of nanoscale laterally structured materials [1].

Different morphologies of quadratic, hexagonal or wave like patterns under oblique or normal incidence were demonstrated using low energy ($E < 5$ keV) ion-bombardment of solid surfaces. The observed structures on the surface are rather well described and explained by the interplay between a roughening process caused by ion beam erosion of the surface and smoothening processes due to thermally or ion-beam induced surface diffusion. Such a pattern can be well explained in terms of the Bradley–Harper model and respective extensions [2].

Recently it was observed [3–5] that irradiation with high energy ions (Ar^{+}, $E > 50$ keV) induces periodical, ripple like, surface structures as well. This surface ripple formation is accompanied by a buried ripple structure at the amorphous-crystalline interface with the same lateral spacing as found at the surface. Using X-ray diffraction it was shown that ripples at the surface are followed by a nearly sinusoidal

[*] Corresponding author: e-mail: j.grenzer@fzd.de, Phone: +49 351 260 3389, Fax: +49 351 260 3438

shaped interface between the strongly damaged, not completely amorphous near-surface region and the crystalline material [4]. In contrast to low energy ion irradiation a periodical buried ripple formation at the amorphous to crystalline interface is restricted to azimuth angles close to the [110] direction, whereas there is no azimuthal dependence for the ripple formation at the sample surface. The crystalline ripple side planes are close to {111} side facets. These narrow fabrication conditions suggest that the erosion process is strongly influenced by the crystal lattice. Although the amorphous and crystalline phases of the irradiated Si are well studied, many features of the mixed and transition regions remain unknown.

Ion beam treatment often is assisted by a subsequent thermal annealing [6] to remove the ion induced damage. Therefore, in this paper we studied the role of temperature on the subsurface morphology of modulated nanostructures and the behaviour of the amorphous-crystalline interface. Annealing can play an important role for the reconstruction of the lattice at the amorphous to crystalline transition.

2 Temperature treatment

The sample was prepared under optimum conditions for the ripple formation using a dose of 5×10^{17} Ar^+/cm^2 at an implantation energy of 60 keV, the ion beam incident angle being 60 degree. Detailed information can be found elsewhere [3, 4]. The surface morphology of the ion-bombarded Si(001) sample was studied using atomic force microscopy that yields an average spatial ripple periodicity of 715 nm and a surface undulation amplitude of 40 nm. The subsurface structure is investigated by grazing incidence X-ray diffraction (GID) and X-ray amorphous scattering (GIAS) using synchrotron radiation. The later experiments have been performed at the ID01 beam line at ESRF [7]. The energy of the incident beam was 8 keV and the scattered signal was collected by a position-sensitive detector. The GID measurements are performed by rocking the sample through an exact in-plane Bragg condition measuring the structure of the crystalline part at the amorphous-crystalline interface. For X-ray amorphous scattering (GIAS) the detector was scanned in-plane in a large angular range of 2θ for a fixed azimuth angle that corresponds to a probing throughout the reciprocal space far away from any reciprocal lattice point. This scans provide information about the damaged top layer. Both measurements are performed under

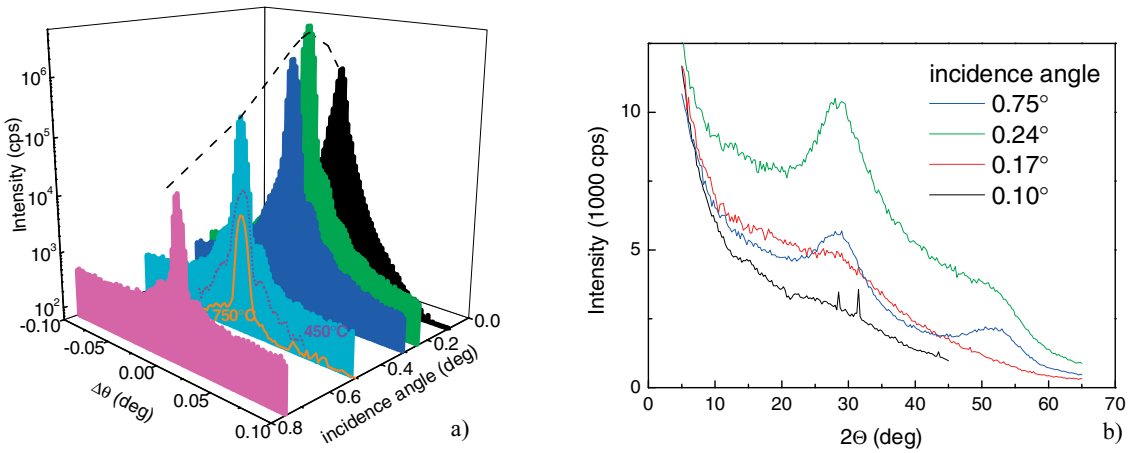

Fig. 1 (online colour at: www.pss-a.com) a) GID curves around (220) Bragg peak of Si(001) substrate for different incidence angles (α_i), i.e. penetration depth. The filled curves are measured before annealing; the dotted line at 450 °C and the solid line at room temperature after annealing up to 750 °C. The dashed curve shows the α_i dependence at Bragg peak position. b) Amorphous scattering as a function of the incidence angle α_i. The broad diffraction maxima refer to the next-neighbour distances of crystalline silicon.

shallow angle of incidence $\alpha_i \approx \alpha_c$, where α_c is the critical angle of total external reflection yielding to a value of 0.23° at 8 keV. The temperature measurement was performed using an evacuated furnace in a temperature range between room temperature and 750 °C.

Figure 1a shows GID patterns taken at different incidence angles α_i, i.e. different penetration depths. It shows the diffraction at the Si(220) Bragg reflection. For large penetration depths >100 nm ($\alpha_i > 0.35°$) a number of satellites measuring the average lateral spacing of the buried ripple structure appeared in addition. These satellites indicate that the crystalline-amorphous interface shows a periodical modulation. The buried ripple wavelength (680 nm) is very close to that one on the surface (715 nm), as it was determined by AFM. The satellites disappear at low penetration depths ($\alpha_i \leq 0.35°$) accompanied by an increase of the full width half maximum of the main Si peak. This is caused by an almost complete loss of the crystalline modulated structure within the damaged near surface region.

The GIAS scans (Fig. 1b) show the defect structure near the rippled surface of the as-irradiated sample. The curve at $\alpha = 0.1°$ is flat but shows two small peaks at $2\theta = 28.5°$ and $2\theta = 31.5°$ originating from tiny crystallites at the sample surface. These angular 2θ positions correspond exactly to (111) and to the forbidden (200) reflections from strained Si crystallites. Such crystallites, sticking at the whole sample surface, are mainly caused by the cleavage process of the wafer prior to ion bombardment [8]. With increasing α_i the scattering pattern of the implanted area is dominated by broad intensity humps with two clearly visible maximum positions on top of a nearly uniform background. Both features are increasing with increase of α_i. The maxima ($2\theta = 28.5°$ and $2\theta = 47.3°$ for 8 keV) correspond to lattice distances of the (111) and (220) net planes but their width indicates that they come from very small clusters diluted in the amorphous matrix [8].

Figure 2 shows the behaviour of the GIAS profiles versus temperature. Qualitatively the profile remains unaffected up to about 450 °C. Both GIAS maxima still exist but changing slightly their intensity ratio. The same holds for the (220) GID pattern (Fig. 1a). The dotted line in Fig. 2a shows that the ripple structure still remains unaffected up to this temperature range. After an increase to 750 °C major changes have been observed in the GIAS scattering pattern for the region close to the (111) peak. The second broad hump at (220) becomes much broader and then completely disappears (Fig. 2a). At the same time the first one transforms to a narrow peak at the (111) position. Over 4 hours at 750 °C the half width of this peak decreases continuously; indicating the onset of a re-growth process. This process is accompanied by a continuously change of the diffraction pattern until a stable system is formed and a sharp (111) reflection appeared (see Fig. 2b). At this high temperature the periodic structure (ripples) at the crystal line-amorphous interface were completely lost (solid line in Fig. 1a). After cooling down to room tem-

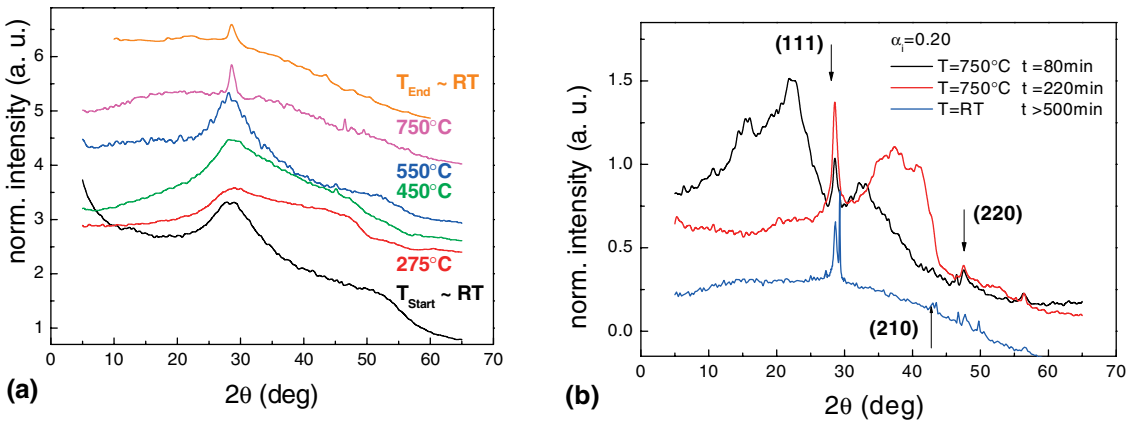

Fig. 2 (online colour at: www.pss-a.com) a) Amorphous scattering at $\alpha_i = 0.3°$ vs. temperature. The broad peak at $2\theta = 28.5°$ refers to the next-neighbour distance of amorphous silicon. The curves are shifted for clarity. b) Amorphous scattering at $\alpha_i = 0.2°$ during and after annealing at 750 °C.

perature the (111) GIAS peaks remains sharp being on top of a smooth broad background, but with a smaller intensity compared to that found at 750 °C. The GIAS scans taken at different incidence angles show a strong modification of the shape of amorphous scattering close to the surface. Additionally, after annealing the GIAS profiles at shallow incidence angles α_i reveal sharp peaks corresponding to different Si reflections (111, 210, 220).

The broad amorphous humps reveal short range ordering in amorphous material [9]. At room temperature the strongest one comes from nearest neighbour distances with a maximum at the position of (111) planes and second hump at (220) planes. Due to annealing at high temperature an interplay of the different processes takes place: a partly recrystallization of damaged material and a future expansion of the near neighbour distances. Such an increase of the shortest neighbour distances causes a shift of GIAS peaks to smaller 2Θ angles. During the first phase of annealing the scattering pattern is still dominated by the amorphous scattering (broad hump at 750 °C at 80 min). With increasing time ($T = 750$ °C at 220 min, Fig. 2b) the scattering signal from the (111) peak (28.5°) grows on the cost of amorphous scattering, thus the amount of crystalline material increases. However, the remaining broad hump confirms that there is still damaged material. Cooling down to room temperature ($t > 500$ min) results in a sharp crystalline peak sitting on top of a broad but low diffuse background. Increasing the resolution of the experiment showed that the Bragg reflections (lowest curve measured after annealing, Fig. 2b) are splitted up, indicating that Si crystallites are partially strained.

3 Ex-situ investigations

Ex-situ AFM inspection after annealing has shown several islands with heights up to 200 nm appearing on top of the amorphous ripples (Fig. 3). Their crystallographic orientation was randomly distributed and did not depend from the underlying Si bulk crystal. They might be grown up either by homoepitaxy from amorphous material or by heteroepitaxy from the small crystallites being on top of the sample surface (see above). Additionally, these islands show a substructure similar to the initial ripple pattern (with the

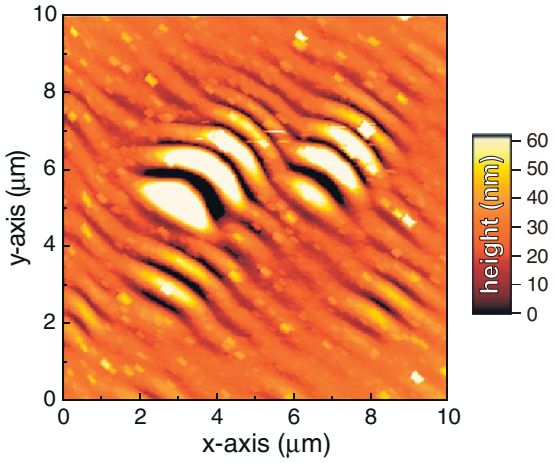

Fig. 3 (online colour at: www.pss-a.com) AFM picture of the rippled sample surface after annealing at 750 °C. We find islands with height up to 200 nm spread over several ripples; AFM pictures of as irradiated samples can be found in [4].

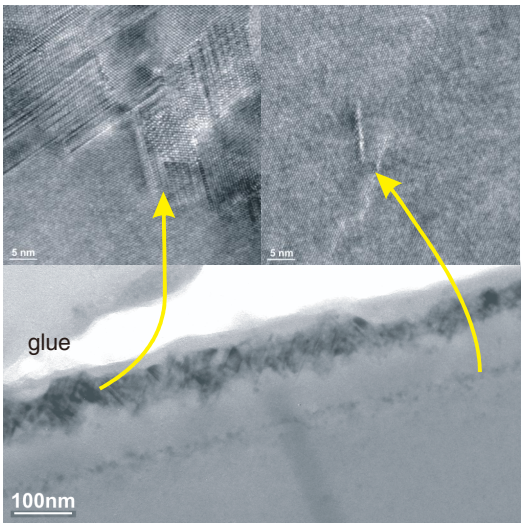

Fig. 4 (online colour at: www.pss-a.com) Cross-section TEM of an annealed (750 °C) sample. In the region of the amorphous ripples twinned Si crystals are grown up (left inset). At a depth of about 200 nm a region of defects is visible (right inset).

same period of about 700 nm) of the obliquely implanted silicon surface. Along the ridges they have an extension of 4 μm. We refer the sharp peaks in shallow GIAS scans to these islands.

During annealing at $T > 700$ °C a second process takes place close to the former buried amorphous-crystalline interface. Figure 4 shows cross-sectional TEM pictures of the annealed sample. Since the as-irradiated samples has shown already small microcrystallites with random orientation at this interface [3] we found, consequently, after annealing large twinned Si nano-crystals grown completely into the former amorphous layer. Excluding almost any swelling this process can be attributed to a polycrystallisation above 700 °C. This process can be understood in the same manner as in [6] by two concurrent processes: an epitaxial regrowth process at the amorphous-crystalline interface and nucleation processes inside the amorphous layer. Additionally, the twin formation might be understood from the strong directional dependence of ripple formation found previously [4, 5]. In fact, we found pronounced crystal truncation rods along [111] and [1 $\bar{1}$1] for this sample prepared under optimum conditions where the side facets of the ripples are close to (111). Therefore we can suggest that these 111 facets act as preferential channels for atomic diffusion.

At the same time the long annealing procedure transforms the defect-rich crystalline region below the former amorphous-crystalline interface again into an almost perfect, defect free material; thickness fringes can be seen easily in TEM. Partially defects originating from this region migrate into a deeper one and form a plane of defects reducing the overall stress inside the crystalline material. Such a plane of defects was not found underneath the not irradiated but annealed silicon surface.

4 Conclusions

Thermal annealing of implanted semiconductors is a standard tool to improve the crystallinity of the prepared samples. In the present case we found a partial recrystallization for a sample irradiated with a high dose of Ar^+ ions (5×10^{17} cm^{-2}) prepared under an ion beam incidence close to [111] direction. We recorded *in-situ* the temperature induced modification of grazing incidence diffraction and amorphous scattering signals allowing us to follow the development of the re-crystallization during annealing.

After annealing at about 750 °C, we found a reduction of the amorphous scattering and an increase of the Si(111) Bragg diffraction intensity indicating a growth of crystalline material. In-situ measurements reveal different processes. At the beginning dominates the GIAS scattering. In the next phase the crystalline scattering prevails mirroring the process of recrystallization and correspondingly the amorphous scattering decreases. The formation of a buried defect-rich region close to the former amorphous-crystalline interface was confirmed by TEM investigations. The formation of strained crystalline islands on top of the former surface ripples was supported by AFM observations. Whereas these crystallites are randomly in azimuthal orientation (as random as these small crystallites before annealing) there are some indications that the ripple morphology, especially the formed (111) side facets at the amorphous-crystalline interface, trigger the growth of twined crystallites into the amorphous layer towards the surface.

This regrowth process was clearly observed by GID and GIAS X-ray techniques. The combination of complementary *in-situ* and *ex-situ* methods afford a detailed evolution of the re-crystallization process itself.

Acknowledgements We would like to thank the beam line ID01 staff for the support at ESRF. This work was supported by the DST-DAAD India–Germany Collaborative Program. This project was supported by the combined DFG grant No GR2085/2-1 and PI217/28-1.

References

[1] U. Valbusa, C. Boragno, and F. Buatier de Mongeot, J. Phys.: Condens. Matter **14**, 8153 (2002).
[2] R. M. Bradley and J. M. E. Harper, J. Vac. Sci. Technol. A **6**, 2390 (1988).
M. A. Makeev, R. Cuerno, and A.-L. Barabasi, Nucl. Instrum. Methods Phys. Res. B **197**, 185 (2002).

[3] T. K. Chini, F. Okuyama, M. Tanemura, and K. Nordlund, Phys. Rev. B **67**, 205403 (2003).
[4] S. Hazra, T. K. Chini, M. K. Sanyal, J. Grenzer, and U. Pietsch, Phys. Rev. B **70**, 121307(R) (2004).
[5] D. P. Datta and T. K. Chini, Phys. Rev. B **71**, 235308 (2005).
[6] S. Matteson, P. Revesz, Gy. Farkas, J. Gyulai, and T. T. Sheng, Appl. Phys. Lett. **51**, 2625 (1980).
[7] http://www.esrf.eu/UsersAndScience/Experiments/SurfaceScience/ID01/
[8] S. Grigorian, U. Pietsch, J. Grenzer, D. P. Datta, T. K. Chini, S. Hazra, and M. K. Sanyal, Appl. Phys. Lett. **89**, 231915 (2006).
[9] R. Zallen, The Physics of Amorphous Solids (Wiley, New York, 1983), p. 251.

